

Investigation of the Microwave Iron-Production Process with Multipoint Pyrometric and Spectroscopic Measurements

Akihiro MATSUBARA, Sadatsugu TAKAYAMA¹⁾, Kazuya NAKAYAMA, Takahiro KANEBA, Masahiro TOMIMOTO, Ryuichi AKIYAMA¹⁾, Shigeki OKAJIMA, and Motoyasu SATO¹⁾

Chubu University, 1200 Matsumoto, Kasugai, Aichi 487-8501, Japan

¹⁾*National Institute for Fusion Science, 322-6 Oroshi, Toki, Gifu 509-5292, Japan*

(Received 19 November 2007 / Accepted 11 February 2008)

Carbothermic reduction of magnetite in a 2.45-GHz microwave multimode furnace was investigated with multipoint pyrometric and spectroscopic measurements. Both experimental results emphasize the importance of surface heating of the specimen by microwave-generated plasma for reducing iron oxide. The pyrometric observation shows a shift of the heating mode from *the direct volumetric heating* by microwave to *the surface heating* by microwave-generated plasma, when the temperature of the material suddenly rises from ~800 to ~1000°C accompanied by light emission from plasma. The emission spectrum in the near-UV range (240-310 nm) changes drastically from a continuous spectrum to a line emission spectrum of iron, representing progress of carbothermic reduction of iron oxide. The multipoint spectroscopic observation indicates extensive carbothermic reduction occurring on the entire upper surface of the specimen.

© 2008 The Japan Society of Plasma Science and Nuclear Fusion Research

Keywords: microwave iron production, carbothermic reduction, direct volumetric heating by microwave, surface heating by microwave-generated plasma, pyrometric measurement, spectroscopic measurement, near-UV emission, continuous spectrum, cathodoluminescence, plasma surface interaction.

DOI: 10.1585/pfr.3.S1085

1. Introduction

Plasma-surface interaction is a crucial issue in fusion research as well as plasma processing; in some cases, it has been also studied in the field of microwave material processing associated with thermally activated processes based on microwave heating [1]. Microwave irradiation enables *direct volumetric heating*. The absorption length of microwaves in the material is comparable to or larger than the scale length of most electrically insulating materials such as ceramics, polymers, and certain composite materials, even metal if it is in a powdered state. In general, it leads to significant energy savings and reduction in process time [1,2]. During microwave irradiation, electric discharge occasionally occurs on the surface of the material, which is promoted by the presence of vapors of various substances [2] and thermal electrons emerging from hot spots on the surface. These electric discharges should be avoided, because a part of microwave energy is absorbed as kinetic energy of plasma electrons, and direct volumetric heating by microwave becomes non-dominant. However, a few applications can also utilize *surface heating* by microwave-generated plasma, in order to modify the surface condition or boost a specific chemical reaction [1]. One such application is microwave iron production presented here.

High-purity pig iron has been produced successfully in a multimode microwave test reactor from powdered iron

ores (magnetite) with carbon as a reducing agent in a nitrogen environment at atmospheric pressure [3]. Microwave iron production has the advantage that CO₂ emissions can be reduced by tens of percents compared with that in conventional blast furnaces, if the electric power for the microwave radiation is generated by renewable energy such as solar, hydro, and nuclear power [4]. A feature of the microwave method is the sudden rise in temperature of the material from ~700 to ~1000°C accompanied by light emission of plasma, called the temperature jump [5]. The reason of the temperature jump is the emergence of an additional energy flow to the material through the plasma.

In situ visible emission spectroscopy has been introduced to demonstrate the characteristics of the heating mechanism including direct volumetric heating by microwave and/or surface heating by plasma [6]. Light emission that occurs after the temperature jump consists of strong atomic/molecular lines. These lines have been well assigned as spectra listed in the spectrum database based on the spark and arc discharge [7], indicating the presence of plasma electrons with electron temperature of several electron volts. It was found that the structure of the emission spectrum in the near-UV range (240-310 nm) changes drastically from a continuous spectrum to a line spectrum of iron with increasing surface temperature [5]. The continuous spectrum was attributed to cathodoluminescence due to the impingement of plasma electrons onto the specimen surface of magnetite. The evolution from a continu-

author's e-mail: Matsubara.Akihiro@sti.chubu.ac.jp

ous spectrum to a line spectrum was the first observation to capture the progress of reduction process of iron oxide by an in situ spectroscopic method.

In a series of experiments concerning the spectral evolution, multipoint spectroscopic and pyrometric measurements were performed to observe the spatial dependence. The spectral evolution presented in a previous article was the result for one sight line of the multipoint spectroscopic measurement [5]. It is expected that the spatial dependence of the spectral evolution will suggest how the reduction process progresses spatially. The homogeneity of the reduction process is related to the efficiency of iron production. The purpose of this article, therefore, is to present the results obtained in those multipoint systems. Both multipoint spectroscopic and pyrometric measurements demonstrate the importance of surface heating of the specimen by microwave-generated plasma for reducing iron oxide.

The experimental setup is shown in Sec. 2. Results and discussion are presented in Sec. 3. First, observations of the heating characteristics of microwave iron production with pyrometric measurements are described in Sec. 3.1. In Sec. 3.2, the reduction process inferred from the observed emission spectrum is presented. A brief summary is given in Sec. 4.

2. Experimental Setup

The multimode test furnace at National Institute for Fusion Science is shown in Fig. 1. According to the concepts developed in Germany to improve the homogeneity of the electromagnetic field, the applicator shape is hexagonal [8]. The furnace is equipped with five magnetrons. The microwave power of one magnetron is 2.5 kW at a frequency of 2.45 GHz. In the experiment reported here, the power of incident microwave is continuous, and its level is 2.5 kW. Two mode stirrers scatter the standing waves. Before starting the process, the chamber was evacuated using

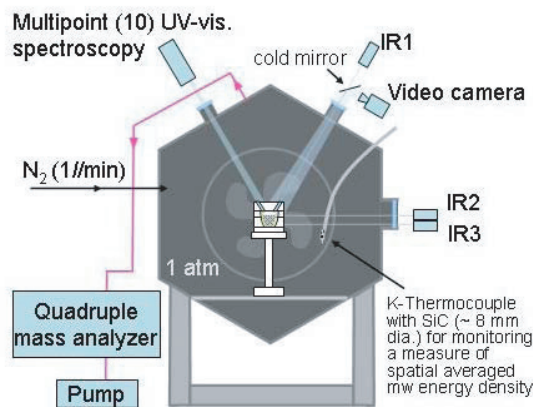


Fig. 1 Schematic diagram of the multi-mode test furnace and diagnostics system. The distance between opposite sides of the hexagonal cross-section is 1.1 m.

a rotary pump and refilled with nitrogen gas. During processing, a continuous nitrogen gas flow of about 1 L/min was used with a pressure a little higher than the ambient pressure.

Figure 2 (a) shows the schematic of the sight lines for the pyrometric and spectroscopic measurements. InGaAs pyrometers [labeled as IR's in Figs. 1 and 2 (a)] record the temperature. IR1, IR2, and IR3 are directed at the specimen surface, the crucible outer surface, and the crucible bottom, respectively. The detection wavelength range for IR1 and IR3 is 1.95-2.5 μm , and that for IR2 is 0.8-1.6 μm . The spot size is 10 mm for IR1, 4 mm for IR2, and 3 mm for IR3.

In the multipoint spectroscopic diagnostic, the light emitted from the material is collected through the viewing port using a magnifying lens located on the top of the furnace. Ten sightlines with a distance of 2.2 mm and a spot diameter of 1.0 mm are provided by means of a fiber bundle and magnifying lens. Seven sightlines, labeled as f1-f7, are directed at the specimen surface through the holes of a insulator board, which acts as the top-cover, and the remaining three (f8-f10) are terminated by the surface of that insulator board. The spectrometer is a Czerny-Tuner imaging polychromator with a focal length of 250 mm. The wavelength resolution is 0.5 nm, and the wavelength range in one frame is 70 nm. The exposure time is 2 s, and the cycle time for capturing is 5 s.

As shown in Fig. 2 (a), IR1 and f1 are adjusted in such a way that their view fields overlap at a point 15 mm above the bottom of the crucible along its central axis. It is noted that the position of the measurement points on the surface (i.e., intersection of the sight lines and the surface of material) moves down with increasing surface temperature, since the powdered material shrinks. This situation is depicted schematically in Fig. 2 (a); the light-shaded and dark-shaded areas indicate the shape of the specimen before and after the microwave irradiation, respectively. Fig.

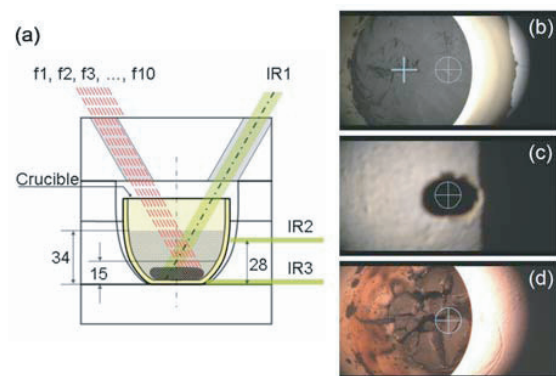


Fig. 2 (a): Sight lines for multipoint spectroscopic observation and configuration of the specimen, crucible, and insulator. (b)-(d): Video camera pictures of the sample surface without top insulator in (b), with top insulator in (c), and after the heating and removing top insulator in (d).

ure 2 (b) shows a photograph of the surface of the material captured by a video camera located above the furnace before microwave irradiation (for location of the video camera see Fig. 1). In Figs. 2 (b)-(d), the circle with cross indicates the field of view of IR1, with a 10-mm diameter. The left cross in Fig. 2 (b) indicates the measurement point on the surface of the specimen for the sight line of f1 at the initial height of the specimen.

The purified reagent, Fe_3O_4 with graphite, was prepared according to the method used in the previous experiment [5]. The mix ratio was $M_{\text{Fe}_3\text{O}_4}:M_{\text{C}} = 90:10$ (= 54.0 g:6.0 g) by weight. Corresponding mol ratio was $n_{\text{Fe}_3\text{O}_4}:n_{\text{C}} = 1.0:2.0$.

3. Results and Discussion

3.1 Heating characteristics observed with pyrometers

The main characteristic of the heating process in microwave iron production is the temperature jump of the surface temperature of the raw material. Figure 3 (h) shows temperature traces obtained for sight lines of IR1, IR2, and IR3. In the trace obtained by IR1 (temperature of the specimen surface), the temperature jump appears at $t = 740\text{--}840$ s. The temperature difference between IR1 and IR3 (temperature of the crucible bottom) is larger for the period after the temperature jump than that for the period before the jump. The temperature jump represents the shift of the heating mode from direct-volumetric heating by microwave to surface heating by microwave-generated plasma.

3.1.1 Before the temperature jump

In the early stage, (the start point of microwave incidence is $t = 34.6$ s) the temperatures of IR1, IR2, and IR3 increase immediately, and a hot spot is observed on the surface of the material. Figure 3 (i) shows photographs of the surface for various steps as heating progresses. The photographs were captured by the video camera with a view field shown in Figs. 2 (b) and (c). Before the temperature jump ($t < 743$ s), the structure of bright hot spots appears continuously on the surface, as shown in the first and second photographs labeled as $t = 140$ and $t = 185$ s, respectively.

The hot spots seem to be distributed along cracks on the surface, and micro-scale discharge sparks often occur along the cracks. The mechanism of generation of the hot spots is not clear, but is possibly related to an instability due to a positive correlation between the absorbance of microwave and the temperature of the material. The thermal energy loss by thermal radiation is smaller for the cracks because of the smaller solid angle of its radiation. If the temperature of cracks increases slightly, the positive correlation can make them grow into hot spots. Another possibility is the effect of the crack structure on microwave propagation along it.

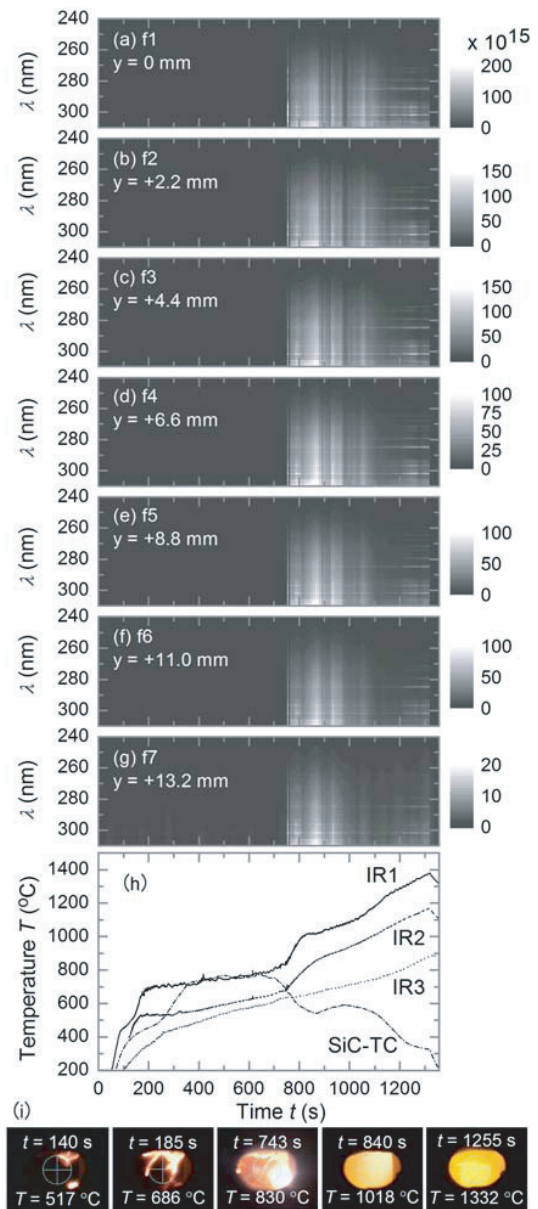


Fig. 3 Time evolution of the emission spectrum for various sight lines (a)-(g). Temperature traces obtained for IR1, IR2, and IR3 (h). The temperature of SiC-TC (see text) is also included in (h). A series of the photograph captured by video camera showing the evolution of the surface condition (see also Fig. 2).

The existence of the hot spot is reflected in the temperature trace. It is noticed that the hot spot enters the field of view for IR1 (depicted by the circle) for the period between the first ($t = 145$ s) and second photographs ($t = 185$ s) of Fig. 3 (i). This corresponds to a rapid increase in the surface temperature for IR1 up to 700°C in the period of $t = 145\text{--}165$ s. Until $t = 700$ s, all temperatures increase moderately, while the crack structure continues along with micro-scale sparks.

3.1.2 After the temperature jump

After $t = 700$ s, the size of spark grows approximately each time it appears (see third picture labeled $t = 743$ s), and finally it triggers a large-scale emission similar to a flame covering the entire top surface (see fourth picture labeled $t = 840$ s). Simultaneously, the increase in temperatures observed by IR1 and IR2 becomes rapid, and an intense emission spectrum begins to appear, which shows typical phenomena of the temperature jump. It is noticed that a much stronger spectrum is detected by f1 at the beginning of the period in which the spectrum appears continuously, showing significant growth of the spark. There is no jumping behavior in the temperature trace obtained by IR3, indicating the heating is mainly due to the plasma generated on the top surface of the specimen.

In Fig. 3 (h) the dashed-dotted line with the label SiC-TC, which indicates the temperature trace for the thermocouple tip covered with the silicon carbide tip (see Fig. 1), represents the relative change in the spatially averaged microwave energy density. The silicon carbide is an absorber of the microwave, and plays a role of a thermometer of electromagnetic field. The temperature of the SiC-TC decreases at the temperature jump, implying the emergence of the plasma being the microwave absorber.

3.2 Reduction process inferred from the emission spectrum

Figures 3 (a)-(g) show the time evolution of the emission spectrum as a contour map for various positions of the sight lines of f1-f7, respectively. The drastic transition from a continuous spectrum to a line emission spectrum is seen for every sight line. As described below, such evolution represents the progress of the reduction process of magnetite. Therefore, the moderate spatial dependence suggests extensiveness of the reduction process.

3.2.1 Spectral evolution

Before the detailed description of the spatial dependence of the spectral evolution, explanation of the spectral evolution is presented first. The transition from a continuous spectrum to a line emission spectrum can indicate the reduction of a magnetite. The temperature range for the transition of the spectrum is typically 1050-1250°C, which is consistent with the result in the previous report [5]. That range is coincident with the temperature range of a high reduction rate for magnetite and wustite [3].

Typical continuous spectrum and line spectra appearing in the evolution are shown in Fig. 4. It should be noted that the spectral intensity of the continuous spectrum is at least three orders of magnitude larger than that of blackbody emission for the present surface temperature of about 1000°C. Almost all the line spectra shown in Fig. 4 (c) are well assigned to the well-known spectra of iron atom observed in arc and spark discharges [7].

The origin of the continuous spectrum has been

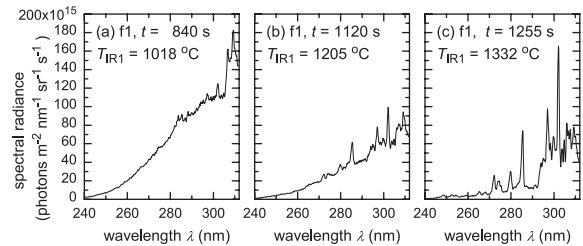


Fig. 4 Emission spectrums appearing in the evolution. The peaks around 308 nm in (a) indicate OH spectrum. Almost all the peaks in (b) and (c) are due to iron atom.

stated to be the cathodoluminescence of magnetite [5]. Cathodoluminescence, a solid-state fluorescence, can be induced by impingement of plasma electrons onto the specimen surface, resulting in the excitation of electrons from the valence band into the conduction band, and de-excitation resulting in broadband emission. The cathodoluminescence of magnetite was studied by Balberg and Pankove [9]. They reported the first luminescence observation in transition-metal oxides and suggested the semi-quantitative band structure of magnetite. They obtained the emission spectrum of the cathodoluminescence showing emission edge beginning at 310 nm and extending to above 620 nm with the main peak at about 480 nm and a sub peak at about 390 nm. In connection with the electric excitation of magnetite, the absorption spectrum for thin films of magnetite showed a 210-620 nm band with a peak wavelength at about 390 nm [10]. The continuous spectrum of the present results coincides with the wavelength range of those luminescence/absorption spectra, although the agreement of the peak wavelength is not clear yet, because the peak of the continuous spectrum is out of the spectral window (higher wavelength side).

The interpretation of the cathodoluminescence of magnetite is supported by another experimental fact that even in the case no graphite powder is mixed in the raw material (i.e., pure magnetite powder only), an identical continuous spectrum was observed [5]; therefore, the continuous spectrum is not attributed to molecular band spectra associated with carbon. Thus, it can be said that the continuous spectrum indicates the existence of magnetite.

3.2.2 Spatial dependence of the spectral evolution

From Figs. 3 (a)-(g), it is found that the decay of the continuous spectrum begins earlier for the larger number of sightline. The detailed difference between spectral evolutions is seen from Figs. 5 (a) and (b) that depicts the time trace of the spectral intensity, I_{SR} , for two sightlines of f1 and f5, respectively (these results are drawn from Figs. 3 (a) and (e)). It should be noted that the measurement point on the surface of the specimen for each sight line moves to the periphery of the material (toward the right hand side of Fig. 2 (a)) with increasing material temperature, because the material shrinks and its height drops

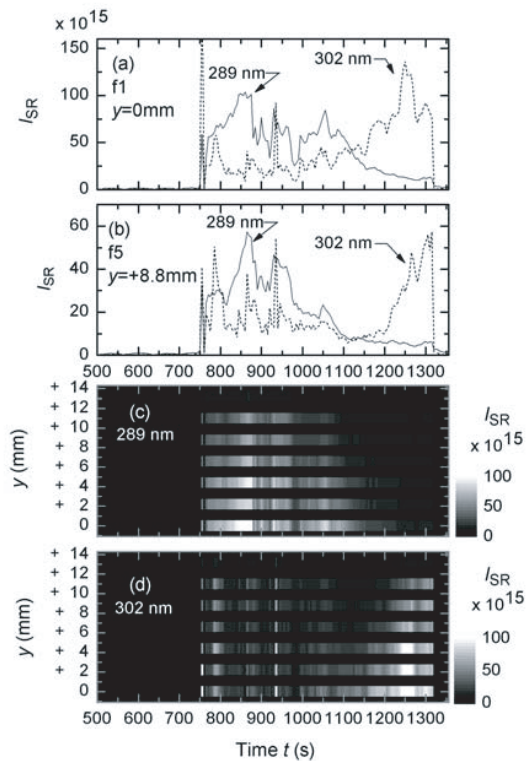


Fig. 5 The time evolution of the spectral intensity, I_{SR} , (spectral radiance in the unit [$\text{photons m}^{-2} \text{s}^{-1} \text{sr}^{-1} \text{nm}^{-1}$]) at the wavelengths of $\lambda = 289$ and $\lambda = 302$ nm for the sight line of f1 ($y = 0$ mm) in (a) and f5 ($y = 8.8$ mm) in (b), and for various position of the sight line as the contour map in (c) for $\lambda = 289$ nm and (d) for $\lambda = 302$ nm.

during heating. Consequently, the spectrum of the sight line with the larger number reflects the emission from the periphery of the specimen more strongly.

The solid line in Fig. 5 (a), which indicates the spectral intensity of the continuous spectrum I_{SR} at $\lambda = 289$ nm for the sight line of f1, decreases clearly from $t \sim 1050$ s. On the other hand, for the solid line in Fig. 5 (b), I_{SR} starts decreasing clearly from $t \sim 950$ s. The start time of the decay of the continuous spectrum exhibits a smooth spatial variation as shown in Fig. 5 (c). The continuous spectrum decays faster near the periphery than near the center of the specimen.

In contrast with the decay of the continuous spectrum, the intensity of the iron spectrum grows. The near central position, I_{SR} for $\lambda = 302$ nm (the dashed line in Fig. 5 (a)) increases moderately. In the value of I_{SR} , the component of the continuous spectrum is already subtracted. In the near periphery, I_{SR} (the dashed line in Fig. 5 (b)) decreases briefly at $t \sim 1100$ s, and then increases rapidly. As shown in Fig. 5 (d), the spatial dependence is smooth.

An explanation of the spatial dependencies of the spectral evolution can be given based on the view that the carbothermic reduction progresses extensively on the surface of the specimen. The preceding decay of the continu-

ous spectrum at the periphery of the specimen suggests that the reduction process is completed earlier at the periphery than at the center of the material. This can result from the concentration of the heat load on the periphery from the plasma, since the upper surface of the specimen is covered with the plasma with size comparable to that of the specimen. This situation is analogous to *field concentration* at the edge.

In order to explain the evolution of the iron spectrum at the periphery (the brief decrease and rapid increases) consistently, another factor is required in addition to the simple view above. This additional factor is evolution of the specimen-shape related to a large-scale crack and melting. It is noted that the spectral intensities of both the continuous spectrum and the iron spectrum decrease in a same manner in the period from $t \sim 1100$ to $t \sim 1150$ s, as shown in Fig. 5 (b). In general, deviation of the sight line from the light source causes a decrease in the spectral intensity independent of the wavelength. Therefore, the brief decrease in the iron spectrum can result from the development of a crack on the specimen surface. According to such consideration of the positional relationship between sight line and light source, the rapid increase in the iron spectrum at the end of heating is explained as follows. It can be considered that the melted portion of specimen spreads outward, and then it returns into the field of view of the sight line. In fact, as shown in Fig. 2 (d), it is seen that there is a crack of 10-mm length and a few-mm width on the periphery of the specimen near the measurement point of the sight line after heating. In addition, a portion of the crack is melted.

4. Summary

The process of carbothermic reduction of magnetite using microwave was investigated experimentally with multipoint pyrometric and spectroscopic measurements. Both results emphasize the importance of surface heating of the specimen by microwave-generated plasma for reducing magnetite. The pyrometric observation shows clearly no sign of the temperature jump at the bottom of the specimen; however, it shows the temperature jump for the upper surface in contact with the plasma generated at the temperature jump. The heating mode shifts from *the direct volumetric heating* by microwave to *the surface heating* by microwave-generated plasma. The spectroscopic observation shows the dynamic evolution of the spectrum from a continuous spectrum to the line spectrum of iron. The continuous spectrum can be attributed to the cathodoluminescence of magnetite. The evolution represents the progress of the reduction process of magnetite. The multipoint spectroscopic observation indicates the extensive carbothermic reduction occurring on the entire upper surface of the specimen. The progress in the evolution of the spectrum is basically faster for the specimens periphery than for its center, which can be due to the concentration of heat load to the edge from the plasma.

Acknowledgment

This research is supported in part by a Grant-in-Aid for Scientific Research on Priority Areas (465) of the Ministry of Education, Culture, Sports, Science and Technology in Japan.

- [1] Committee on Microwave Processing of Materials, *MICROWAVE PROCESSING OF MATERIALS* (National Academy Press, Washington, D.C., 1994).
- [2] Yu. V. Bykov, K.I. Rybakov and V. E. Semenov, *Phys. D: Appl. Phys.* **34**, R55 (2001).
- [3] K. Ishizaki, K. Nagata and T. Hayashi, *ISIJ* **46**, 1403 (2006).
- [4] K. Nagata, K. Ishizaki, M. Kanazawa, T. Hayashi, M. Sato, A. Matsubara, S. Takayama, O. Motojima, D. Agrawal, R. Roy, *Proc. 11th International Conference on Microwave and High Frequency Heating*, (3-6 Sep 2007, Oradea, Romania) pp. 87-90.
- [5] A. Matsubara, S. Takayama, S. Okajima and M. Sato, *textitProc. 11th International Conference on Microwave and High Frequency Heating*, (3-6 Sep 2007, Oradea, Romania) pp. 372-375; A. Matsubara, S. Takayama, S. Okajima and M. Sato, submitted to JMPEE.
- [6] M. Sato, A. Matsubara, S. Takayama *et al.*, *Proc. 10th International Conference on Microwave and High Frequency Heating*, (11-15 Sep 2005, Modena, Italy) pp.272-275.
- [7] NIST Atomic Spectra Database 2007, <http://www.physics.nist.gov/PhysRefData/ASD/index.html>; R.W.B. Pearse and A.G. Gaydon, *The Identification of molecular spectra*, (John Wiley & Sons, Inc., New York 1976); F. Phelp, *MIT Wavelength Table Vol. 2, wavelength by element*, (MIT Press, Cambridge, Massachusetts, London, England, 1982).
- [8] L. Feher and G. Link, DE-PS 19633245C1 (27.11.1997); L. Feher, V. Nuss, T. Seitz, and A. Flach, DE-PS 10329411 (31.1.2005).
- [9] I. Balberg and J.I. Pankove, *Phys. Rev. Lett.* **27**, 1371 (1971).
- [10] P.A. Milles, W.B. Westphal and A. von Hippel, *Rev. Mod. Phys.* **29**, 279 (1957).